

A Comparative Study of Toluene Oxidation on Different Metal Oxides

Marina Duplančić*, Vesna Tomašić, Stanislav Kurajica, Iva Minga, Karolina Maduna Valkaj

University of Zagreb, Faculty of Chemical Engineering and Technology, Marulićev trg 19, Zagreb, Croatia

Contact email address:

marina.duplancic@fkit.hr

ABSTRACT

This work reports the results of experimental and theoretical investigation of toluene oxidation on different metal oxide based catalysts (manganese oxide, MnO_x , mixed manganese-iron oxide, MnFe , perovskite-type manganese oxide, LaMnO_3 and commercial $\text{Pt-Al}_2\text{O}_3$ catalyst). Particular attention was devoted to single and mixed manganese based oxides and ceria based materials as alternatives to conventionally used noble metal containing catalysts.

Toluene oxidation was performed under steady-state conditions in an integral fixed bed reactor operating over a wider range of reaction temperatures and at various space times. The influence of reaction variables on the rate of toluene oxidation was examined using the simple first-order kinetic model and the one-dimensional (1D) pseudo-homogeneous model to describe the reaction system. The proposed model was verified comparing the theoretical predictions with the experimental laboratory results.

The results of catalytic tests indicated that the mixed manganese-iron oxide (MnFe) exhibited remarkable catalytic activity for the toluene oxidation, almost comparable with the activity of the commercial $\text{Pt-Al}_2\text{O}_3$. The reaction temperature T_{50} corresponding to 50% of the toluene conversion was observed at 419 K for the MnFe oxide and at 405 K for the $\text{Pt-Al}_2\text{O}_3$. A very good agreement of experimental data with the proposed 1D model was obtained. Based on the shape of the light-off curve and the values of the apparent activation energies, which decreased from 120.36 kJ/mol to 16.88 kJ/mol with reaction temperature increase, it was concluded that the reaction rate was probably limited by the mass transfer, no matter the relatively small catalyst particle size fraction employed in this study (315 – 400 μm).

1. Introduction

Every year, large amounts of volatile organic compounds (VOCs) are emitted into the air, from both natural and anthropogenic sources and harms human health and our environment. Therefore, control of VOCs emission into the environment become one of the priorities of environmental catalysis. Catalytic oxidation is the preferred technology for abatement of relatively low VOCs concentrations (~ 10 ppm v).

According to the literature, effective heterogeneous catalysts for the VOCs oxidation are either supported noble metal or transition metal oxides (Okal and Zawadski, 2009; Morales et al., 2006). Generally, noble metals are more active, but more expensive than transition metals.

*The article was originally published in the journal "Chemical Engineering Transactions" 57 (2017) 889-894 by the publisher AIDIC Servizi S.r.l. DOI: 10.3303/CET1757149

Among the transition metal oxides, manganese oxides (MnO_x) are reported to be very efficient in catalytic oxidation, since they contain various types of labile oxygen, which are necessary to complete the catalytic redox cycle (Morales et al., 2006). Several metal oxides, especially ceria-based materials have been investigated and it has been observed that may exhibit interesting activity for the VOCs and CO oxidation (Piumetti et al., 2016; Wang et al., 2016). High activity of ceria (CeO_2) mostly originates from the remarkable ability of ceria to store and release oxygen depending on the formation of oxygen vacancies (Pérez et al., 2014). The multi-component catalysts are quite often used in heterogeneous catalysis, since active phases (and promoters) may interact with each other. This may have a beneficial effect on the structural and electronic properties of the catalyst, thus improving their oxidation activity and thermal durability (Vedrine, 2014). Several authors have used perovskite-structured mixed metal oxides with general formula ABO_3 as catalysts for VOC oxidation (Zhang et al., 2014; Stege et al., 2011).

In this work different metal oxides (MnO_x , MnFe , perovskite LaMnO_3 and nanocrystalline CeO_2) were synthesized and their catalytic activities were tested for the toluene oxidation. The most efficient catalyst for toluene oxidation was chosen based on the exhibited activities of the prepared catalysts in comparison to the commercial $\text{Pt-Al}_2\text{O}_3$ catalyst, taking into account the T_{50} (temperature corresponding to 50 % of toluene conversion) and T_{90} (temperature corresponding to 90 % of toluene conversion) values. Finally, the one-dimensional (1D) pseudo-homogeneous model was proposed to describe catalytic oxidation of toluene over the most active catalyst prepared in this study.

2. Experimental

2.1 Catalyst synthesis and characterization

The powder MnO_x and mixed MnFe oxide based catalysts were synthesized by the (co)precipitation method, starting with aqueous solutions of the transitional metal nitrates (e.g. $\text{Mn}(\text{NO}_3)_2 \cdot 4\text{H}_2\text{O}$, $\text{Fe}(\text{NO}_3)_3 \cdot 9\text{H}_2\text{O}$) using modified procedure described previously in the literature (Morales et al., 2006). Nanocrystalline ceria, CeO_2 was prepared by means of hydrothermal process using $\text{Ce}(\text{SO}_4)_2 \cdot 3\text{H}_2\text{O}$ and NaOH as precursors, the details of the procedure have been described previously (Kurajica et al., 2016). Perovskite-type of catalyst, LaMnO_3 was prepared by the citrate method using stoichiometric amounts of an aqueous solution of the metal nitrates (e.g. $\text{La}(\text{NO}_3)_3 \cdot 6\text{H}_2\text{O}$ and $\text{Mn}(\text{NO}_3)_2 \cdot 4\text{H}_2\text{O}$) in the presence of citric acid ($\text{C}_6\text{H}_8\text{O}_7 \cdot \text{H}_2\text{O}$) (Zhang et al, 2014.). All catalysts were calcined at 773 K before catalytic activity evaluation in toluene oxidation.

The prepared catalysts were characterized by X-ray powder diffraction (XRD) and Fourier transform infrared (FTIR) spectroscopy. The powder X-ray diffraction (XRD) was accomplished using Shimadzu diffractometer XRD 6000 with $\text{CuK}\alpha$ radiation. Data were collected between 10 and 70 $^\circ 2\theta$, in a step scan mode with steps of 0.02 $^\circ$ and counting time of 0.6 s. The morphology of the catalytic samples was analyzed on Vega 3 Tescan scanning electron microscope. FTIR spectroscopy experiments were performed on a PerkinElmer[®] Spectrum One FTIR spectrometer. Sample scans were collected with a spectral range from 400 to 4000 l/cm with step of 4 l/cm .

2.2 Catalytic activity tests

Catalytic oxidation of a model VOC pollutant, toluene, over 0.05 g of each catalyst described in Section 2.1 was carried out in a conventional fixed bed reactor in the temperature range of 373 K to ca. 700 K and at various space times. The gas mixture consisted of toluene in nitrogen (242 ppm of toluene in nitrogen, DOL Group, Monza, Italy) and air as an oxidant (Messer). Space times were changed varying the total flow rate of the gas mixture (20-140 cm³/min) over a constant amount of catalyst. The catalyst was placed in the middle of the reactor between two quartz wool plugs. The reaction temperature was regulated by a thermo-controller (TC208 Series) connected to the K-type thermocouple placed within a concentric thermowell inside the reactor and the heaters around the reactor. Reaction was carried out at constant inlet concentration of toluene and at constant ratio of toluene and oxidant (air). The gas mixture was controlled using the mass flow controllers (Brooks). The reactor effluent was analysed before and after reaction using an on-line gas chromatograph (Shimadzu GC-2014) equipped with a flame ionization detector (FID) and a Carbowax 20M column.

2.3 One dimensional mathematical model

In the second part of this study a one dimensional (1D) pseudohomogeneous model was applied to represent the steady-state operation of the fixed-bed reactor used for the low temperature toluene oxidation over MnFe catalyst. Under conditions of the high flow velocity of the reaction mixture and small catalyst particles size (315 - 400 μm) the following assumptions are taken into account in the model development: the plug flow and steady-state conditions, negligible resistance to the interphase mass transfer and chemical oxidation of toluene that can be approximated by the first order reaction (Everaert and Baeyens, 2004). Isothermal conditions were adopted as additional hypothesis, because of the high dilution of toluene in the inlet stream and a small amount of heat generated by the reaction.

Based on these assumptions the reactor and the first order kinetic model were represented by the following equations:

$$-u \cdot \frac{dc_A}{dz} = f(c_A) = r_A^s \cdot \rho_b \quad r_s \cdot \rho_b = f(c_A^s) = k \cdot c_A^s \quad (1)$$

where the rate of reaction per unit mass of catalyst, r_A^s , is associated with the bulk density of the catalyst, ρ_b , in order to ensure the consistency of the dimensions.

After introducing dimensionless variables, given by Eq. (2):

$$y_A = c_A / c_{A0} \quad (2)$$
$$\tau = \tau^* / \tau_{\max}^*$$

the model equations were transformed into dimensionless form:

$$-\frac{dy_A}{d\tau} = \tau_{\max}^* \cdot \rho_b \cdot k \cdot y_A \quad r_s \cdot \rho_b = k \cdot y_A^s \quad (3)$$

and the appropriate boundary conditions at the reactor inlet were given by the following equations:

$$\tau = 0, y_{A0} = 1, y_A^s = 1 \quad (4)$$

Parameter estimation (the rate constant, k) was performed using a modified differential method of data analysis and the Nelder-Mead method of non-linear optimization. The mean square root of differences between the experimentally measured concentrations of toluene and theoretical values provided by the model was used as the correlation criteria (SD).

3. Results and discussion

3.1 Physico-chemical properties of the prepared catalyst

Figure 1 shows XRD patterns of MnO_x , MnFe , CeO_2 and LaMnO_3 catalysts. Diffraction pattern of MnO_x catalyst reveals the presence of two manganese oxides, $\alpha\text{-Mn}_2\text{O}_3$ (ICDD PDF No. 73-1826) and $\alpha\text{-MnO}_2$ (ICDD PDF No. 44-0141). It is obvious that $\alpha\text{-Mn}_2\text{O}_3$ is the major phase while $\alpha\text{-MnO}_2$ could be classified as a minor phase. Narrow $\alpha\text{-Mn}_2\text{O}_3$ diffraction peaks point out to large crystallite size while broad and faint $\alpha\text{-MnO}_2$ are consequence of poorly crystallized phase having small crystallites.

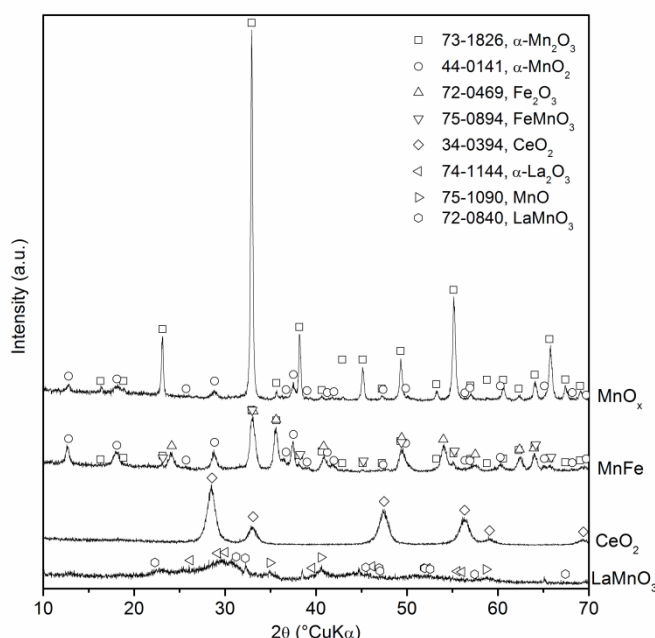


Figure 1. XRD patterns of the prepared catalysts thermally treated at 773 K

Diffraction pattern of MnFe catalyst is the most complex one displaying at least three and possibly four phases. There is no doubt that $\alpha\text{-MnO}_2$ and Fe_2O_3 (ICDD PDF No. 72-0469) phases are present, but additional peaks observed in diffraction pattern could be attributed to both, $\alpha\text{-Mn}_2\text{O}_3$ or FeMnO_3 (ICDD PDF No. 75-0894). Both of those phases have diffraction peaks at similar angles having similar intensities, which is a consequence of the same structure and close Mn^{3+} and Fe^{3+} radii. Additionally, peaks that can be attributed to those phases are weak and occasionally overlapped with the peaks of the main phases. Also, the possibility of the solid solution formation also can't be ruled out. Therefore, based on displayed pattern it could be stated that at least one of them and possibly both, or their solid solution are present in the sample. Diffraction pattern of the CeO_2 catalyst is the simplest one since this sample is pure ceria (ICDD PDF No. 34-0394). The peaks are extremely broad pointing out to very small crystallite size. Finally, LaMnO_3 catalyst is characterized with very weak and poorly resolved diffraction peaks. Based on this pattern it could

be speculated that the sample is composed of at least three poorly crystallized phases, α - La_2O_3 (ICDD PDF No. 74-1144), MnO (ICDD PDF No. 75-1090) and LaMnO_3 (ICDD PDF No. 72-0840).

Fourier Transform Infrared Spectroscopy (FTIR) analysis was performed to compare the chemical composition of the fresh (unused) and used MnFe catalyst. The spectrum (Figure 2) confirmed that there was no significant adsorption of the reactants or possible reaction intermediates (e.g. benzaldehyde or benzoic acid) on the surface of the catalyst during the long-term toluene oxidation over MnFe catalyst. The peak at 1368 1/cm (M-O rocking in plane) implies the presence of metal-oxide group in the catalyst and the peaks at 1736 1/cm (C=O or M-H stretching) and at 1228 1/cm (C-O stretching) can be attributed to some nitrogen or carbon containing molecules probably adsorbed during the catalyst preparation.

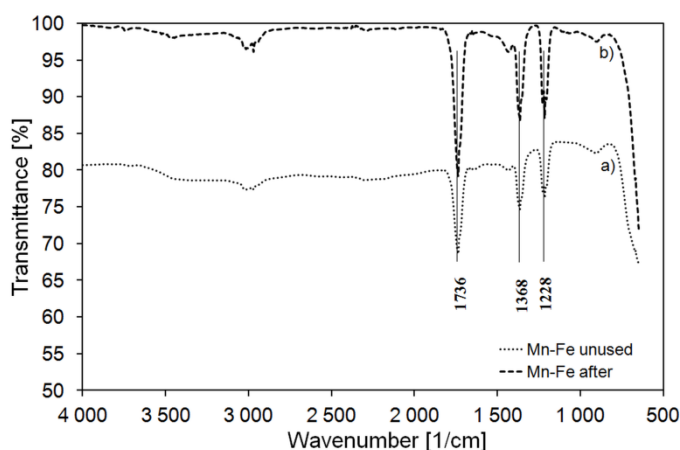


Figure 2. FTIR spectra: a) fresh (unused) MnFe catalyst, b) MnFe catalyst after long-term usage.

3.2 Catalytic performance for toluene oxidation

Toluene, used in this study as a model VOC pollutant, is quite often studied owing to its chemical stability and highly toxic potential (da Silva et al., 2016).

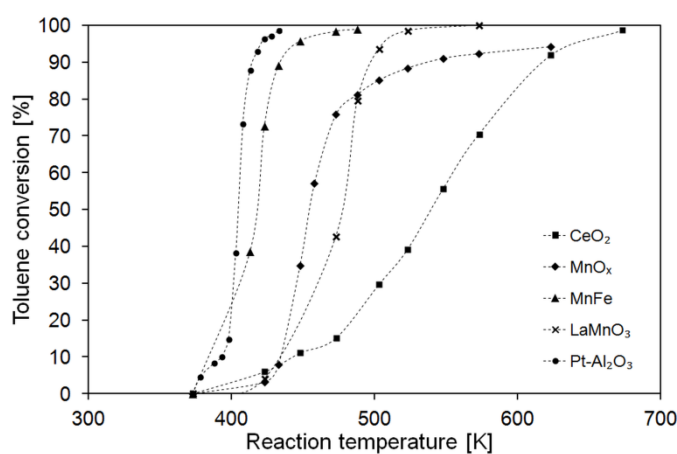


Figure 3. Light-off curves of toluene oxidation as a function of reaction temperature over different catalysts.

Figure 3 summarizes the toluene conversion values over different catalysts as a function of the reaction temperature. The characteristic sigmoidal light-off curves are obtained, which usually

appears in the catalytic systems related to the oxidation of CO, hydrocarbons and similar reaction systems. Among the set of the prepared catalysts, the mixed manganese-iron oxide, MnFe outperforms the other oxides, exhibiting catalytic performance comparable to the performance of the well-known commercial Pt-Al₂O₃ catalyst. Comparison of the results observed for pure MnO_x and mixed MnFe oxide indicates a beneficial effect produced by the incorporation of iron into manganese oxide to activate toluene at lower temperatures during the catalytic oxidation. To compare catalytic activities of different catalysts, the T₅₀ (temperature corresponding to 50 % of toluene conversion) and T₉₀ (temperature corresponding to 90 % of toluene conversion) of toluene over the catalysts were estimated from the Figure 3 and displayed in Table 1. In terms of T₅₀ the following increasing order of activity can be drawn: CeO₂ < LaMnO₃ < MnO_x < MnFe < Pt-Al₂O₃. According to the literature, cerium improves the catalytic role of manganese in toluene oxidation (Pérez et al., 2014; Kim et al., 2008). Although the catalytic performance of CeO₂ in toluene oxidation was less than that of the manganese based catalysts, our future studies will be focused on preparation and more detailed examination of ceria-manganese based mixed oxides and related materials deposited on the metallic substrate with controlled structures and morphologies for enhanced performance in the catalytic oxidation of toluene and other VOCs.

Table 1. T₅₀ and T₉₀ values for studied catalysts

	CeO ₂	MnO _x	MnFe	LaMnO ₃	Pt-Al ₂ O ₃
T ₅₀ [K]	540	455	419	479	405
T ₉₀ [K]	619	535	433	498	415

3.3 Mathematical model results

A one dimensional (1D) pseudohomogeneous model described in Section 2.3 was applied to model the low temperature toluene oxidation over MnFe catalyst. Based on the described assumptions the developed mathematical model was applied and the results are presented as comparison of values obtained by the proposed model and experimental data obtained in the fixed bed reactor for toluene oxidation at different temperatures, shown in Figure 4(a), and as the estimated values of the rate constant, k and the mean square deviations, SD, given in Table 2.

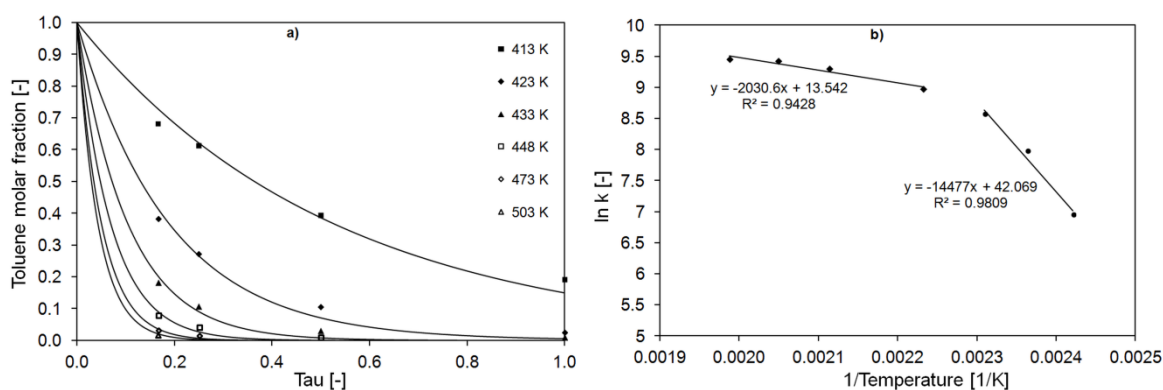


Figure 4. Comparison between experimental data (points) and the values predicted by proposed model (lines) over MnFe oxide at different temperatures (a) and Arrhenius plots for determination of the apparent activation energies, E_a (b).

Table 2. Estimated values of the rate constants, the mean square deviations, SD, the apparent activation energies, E_a and frequency factors, Ar.

T [K]	k [1/min]	SD·10 ³	
413	1044.48	12.19	Ar=1.863·10 ¹⁸ l/min
423	2904.76	10.72	E_a = 120.36 kJ/mol
433	5256.96	6.89	
448	7901.82	3.39	Ar=760704.31 l/min
473	10909.25	2.73	E_a = 16.88 kJ/mol
488	12368.80	1.33	
503	12725.25	0.62	

As can be seen at Figure 4(a), a satisfactory degree of correlation was established. The agreement between the predicted and experimental data supports the ability of the proposed model to describe the experimental system used in this work. Figure 4(b) shows Arrhenius plots used for determination of the apparent activation energies. As it can be seen, unusual Arrhenius plots are obtained corresponding to the apparent energies of activation, which decreased from 120.36 kJ/mol in the lower temperature range (413 - 433 K) to 16.88 kJ/mol in the higher temperature range (448 - 503 K). The explanation of such observations is usually the change in the reaction mechanism or the transition from kinetic to mass-transfer limited reaction regime.

4. Conclusions

A set of metal oxide catalysts prepared by different methods were tested for the toluene oxidation reaction and compared to well-known commercial Pt-Al₂O₃ catalyst. Temperatures at which 50 and 90 % toluene conversion occurs were taken as indices of the catalytic activity (T_{50} and T_{90}). The following increasing oxidation activity order (measured in terms of T_{50} values) was observed: CeO₂ < LaMnO₃ < MnO_x < MnFe < Pt-Al₂O₃ indicating that the mixed manganese-iron based catalyst, MnFe exhibits much better catalytic activity for toluene oxidation than the MnO_x and, most importantly, its catalytic activity was almost comparable to the activity of the commercial Pt-Al₂O₃. The activity of MnFe was found to be superior to single MnO_x, highlighting the promoting effect of iron. A 90 % toluene conversion was observed at 433 K (T_{90}) and complete oxidation was obtained at about 475 K over MnFe catalyst. The agreement between the values predicted by 1D pseudohomogenous model and experimental data supports the ability of the proposed model to describe the experimental system used in this work. The values of the apparent activation energies were determined, which decreased from 120.36 kJ/mol to 16.88 kJ/mol with increasing reaction temperature, indicating that the reaction rate was probably limited by the mass transfer at higher reaction temperatures (448 - 503 K).

References

da Silva, A. G. M., Fajardo, H. V., Balzer, R., Probst, L. F. D., Prad, N. T., Camargo, P. H. C., Robles-Dutenhefner, P. A. (2016). "Efficient ceria-silica catalysts for BTX oxidation: Probing the catalytic performance and oxygen storage", *Chemical Engineering Journal*, 286, 369-376; DOI: 10.1016/j.cej.2015.10.097

- Everaert, K., Baeyen, J. (2004). "Catalytic combustion of volatile organic compounds", *J. Hazard. Mater.*, B109, 113-139
- Kim, H.J., Choi, S.W., Inyang, H.I. (2008). "Catalytic oxidation of toluene in contaminant emission control systems using Mn-Ce/gamma-Al₂O₃", *Environmental Technology*, 29, 559-569; DOI: 10.1080/09593330801984597
- Kurajica, S., Minga, I., Guliš, M., Mandić, V., Simčić I. (2016). "High surface area ceria nanoparticles via hydrothermal synthesis experimental design", *Journal of Nanomaterials*, 1-8; DOI: 10.1155/2016/7274949
- Morales, M.R., Barbero, B.P. (2006). "Total oxidation of ethanol and propane over Mn-Cu mixed oxide catalysts", *Applied Catalysis B: Environmental* 67, 229-236.; DOI: 10.1016/j.apcatb.2006.05.006
- Okal, J., Zawadzki, M. (2009). "Catalytic combustion of butane on Ru/ γ -Al₂O₃ catalysts", *Appl. Catal. B* 89, 22-32.
- Pérez, A., Molina, R., Moreno, S. (2014). "Enhanced VOC oxidation over Ce/CoMgAl mixed oxides using a reconstruction method with EDTA precursors", *Applied Catalysis A: General* 477, 109-116; DOI: 10.1016/j.apcata.2014.03.011
- Piumetti, M., Bensaid, S., Fino, D., Russo, N. (2016). "Nanostructured ceria-zirconia catalysts for the CO oxidation: Study on surface properties and reactivity", *Applied Catalysis B: Environmental*, 197, 35-46; DOI: 10.1016/j.apcatb.2016.02.023
- Stegé, W.P., Cadus, L.E., Barbero, B.P. (2011). "La_{1-x}Ca_xMnO₃ perovskites as catalysts for total oxidation of volatile organic compounds", *Catalysis Today*, 172(1), 53-5.; DOI: 10.1016/j.cattod.2011.02.062
- Vedrine, J.C. (2014). "A Revisiting active sites in heterogeneous catalysis: Their structure and their dynamic behaviour", *Applied Catalysis A: General*, 274, 40-50; DOI: 10.1016/j.apcata.2013.05.029
- Wang, L., Wang, Y., Zhang, Y., Yu, Y., He, H., Qin, X., Wang, B. (2016). "Shape dependence of nanoceria on complete catalytic oxidation of o-xylene", *Catalysis Science & Technology*, 6, 4840-4848; DOI: 10.1039/C6CY00180G
- Zhang, C., Guo, Y., Guo, Y., Lu, G., Boreave, A., Retailleau, L., Baylet, A., Giroir-Fendler, A. (2014). "LaMnO₃ perovskite oxides prepared by different methods for catalytic oxidation of toluene", *Appl. Catal. B Environ.*, 148-149, 490-498; DOI: 10.1016/j.apcatb.2013.11.030